

A Hybrid Measurement Approach for Wideband Characterization and Modeling of Power Transformers

Bjørn Gustavsen, *Senior Member, IEEE*

Abstract—This paper describes a hybrid procedure for wideband characterization and modeling of power transformer behavior from frequency sweep measurements. The approach is based on measuring corresponding sets of voltage and current vectors that are associated with short circuit and open circuit conditions. These vectors are stacked side-by-side in two matrices which are used for computing the short circuit admittance matrix. This hybrid approach is shown to give more information about the transformer behavior than the traditional approach of measuring the admittance matrix directly under short-circuit conditions, which tends to corrupt the small eigenvalues associated with open-circuit conditions. From the obtained admittance matrix, a pole-residue model is extracted via vector fitting and passivity enforcement, thereby giving a model ready for EMTP simulation. The accuracy of the small eigenvalues is retained by using a modal formulation in the fitting and passivity enforcement step. Application to a distribution transformer shows that the hybrid approach can greatly improve the accuracy of time-domain simulations involving high-impedance terminations.

Index Terms—Frequency dependency, passivity, rational model, state-space model, transformer, vector fitting.

I. INTRODUCTION

THE simulation of electromagnetic transients in power systems [1] requires to model all relevant parts of the system with adequate accuracy over a wide band of frequencies. The power transformer is particularly difficult to model since its terminal behavior is highly complex with many resonance peaks in its admittance and voltage ratio. In addition, non-linear core effects greatly affect the transformer behavior [2], [3] although they can normally be ignored when the focus is on high-frequency transients.

Several high-frequency transformer models have been proposed. They are derived from either a detailed description of the transformer geometry and material properties [4]–[8] or from measurements on the transformer terminals [9]–[14]. In this paper we consider the latter approach which requires to measure a set of responses that fully characterize the behavior

of the transformer as seen from its terminals. The measurements have traditionally been based on frequency sweep measurements of the terminal admittance matrix [10]–[13] which is subjected to fitting with rational functions. The rational model leads to highly efficient time-domain simulations via recursive convolution [15] or usage of a lumped circuit equivalent [10]. In practice, it is often desirable to start the simulation from power frequency (50/60 Hz) steady state conditions, followed by a transient event. The correct (linear) behavior at 50/60 Hz can be included in the model by extending the frequency sweep measurement down to 50 Hz as in [12], [13]. At low frequencies, however, the common practice of directly measuring the (short circuit) admittance matrix via frequency sweep measurements gives a model which tends to be highly inaccurate in open circuit applications. This is because the information of the (small) open circuit currents are easily lost in the (large) short circuit currents.

In this paper, we show a procedure for extending the measurement and modeling down to 50 Hz which alleviates much of the difficulties with pure short circuit measurements. This is achieved by combining the short circuit measurements with a set of open circuit measurements. The combined set is used for calculating an admittance matrix which retains the information of both short circuit and open circuit conditions. Using rational approximation by modal vector fitting [17] and passivity enforcement by modal residue perturbation [19], [20], a stable and passive wideband model is obtained for the transformer. The advantages of the new approach are demonstrated in the frequency domain and by comparison with measured time-domain responses.

II. EXISTING MEASUREMENT APPROACHES

A. General

We consider the transformer as a general n -port terminal device with port voltages v and currents i , see Fig. 1. When assuming linearity, the behavior of the transformer at a given frequency can be defined by n linearly independent voltage applications $\{\mathbf{v}_1, \dots, \mathbf{v}_n\}$ and the resulting n current responses $\{\mathbf{i}_1, \dots, \mathbf{i}_n\}$. When these vectors are stacked into matrices \mathbf{V}_n and \mathbf{I}_n respectively, we obtain the identification problem

$$\mathbf{I}_n = \mathbf{Y}\mathbf{V}_n \quad (1)$$

with

$$\mathbf{I}_n = [\mathbf{i}_1 \quad \mathbf{i}_2 \dots \mathbf{i}_n] \quad (2)$$

$$\mathbf{V}_n = [\mathbf{v}_1 \quad \mathbf{v}_2 \dots \mathbf{v}_n]. \quad (3)$$

Manuscript received October 08, 2009; revised December 31, 2009. First published May 18, 2010; current version published June 23, 2010. This work was supported in part by the Norwegian Research Council (PETROMAKS Programme) and in part by Aker Solutions, Compagnie Deutsch, FMC Technologies, Framo, Nexans, Oceaneering Multiflex, Petrobras, Siemens, StatoilHydro, Total, and Vetco Gray. Paper no. TPWRD-00755-2009.

The author is with SINTEF Energy Research, Trondheim N-7465, Norway (e-mail: bjorn.gustavsen@sintef.no).

Color versions of one or more of the figures in this paper are available online at <http://ieeexplore.ieee.org>.

Digital Object Identifier 10.1109/TPWRD.2010.2043747

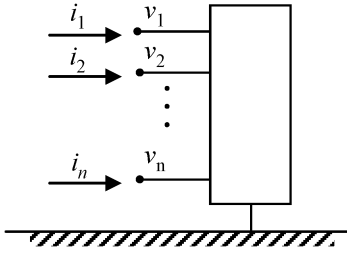


Fig. 1. Transformer terminal voltages and currents.

B. Short Circuit Measurements (Conventional Method)

In the traditional measurement approach [10], [11], the voltage application matrix \mathbf{V}_n is chosen equal to the identity matrix and so the current response matrix \mathbf{I}_n becomes equal to the admittance matrix \mathbf{Y} . This measurement procedure has the advantage that the measurements can be carried out using a conventional vector network analyzer (VNA) with a single output terminal, since the zeros in \mathbf{V}_n are achieved by grounding the associated terminals. The disadvantage of the approach is that small eigenvalues of \mathbf{Y} are easily lost in the measurements.

C. Short-Circuit Measurements With Incorporation of Measured Voltage Ratios

The accuracy of the measurements can be improved by combining the measured \mathbf{Y} with measured voltage ratios [12]. The combined \mathbf{Y} correctly preserves the voltage ratio of the model with one winding open-circuited, but it fails to accurately represent the low-frequency admittance matrix seen into the energized winding. As a consequence, the small eigenvalues of \mathbf{Y} remain corrupted at low frequencies.

D. Modal Measurements

In the modal measurement approach [14], the voltage applications \mathbf{V}_n are taken as the eigenvectors of \mathbf{Y} which are identified by an iterative procedure. With that approach the modes of \mathbf{Y} are excited individually and so a highly accurate characterization of the transformer is in principle possible. The disadvantage is mainly that the approach requires a special VNA with several output terminals that can be controlled individually. Such VNAs are not commercially available although the application of the procedure is available as a service [16].

III. HYBRID MEASUREMENT APPROACH

A. Short-Circuit and Open-Circuit Measurements

We now introduce a new characterization procedure which gives a much more accurate representation of the small eigenvalues of \mathbf{Y} than the conventional approach while at the same time only a single output VNA is needed for the measurement. This is achieved by a little physical insight, noting that the small eigenvalues in \mathbf{Y} are associated with open-circuit conditions while the large eigenvalues are associated with short circuit conditions. Thus, by combining short-circuit and open-circuit measurements one can achieve an improved characterization of

the transformer. The procedure is explained for a two-winding transformer, i.e. for six terminals. We will assume a terminal numbering as defined by (4) where ‘‘H’’ and ‘‘L’’ denote the high-voltage (HV) and low-voltage (LV) side, respectively.

$$\begin{bmatrix} \mathbf{i}_H \\ \mathbf{i}_L \end{bmatrix} = \mathbf{Y} \begin{bmatrix} \mathbf{v}_H \\ \mathbf{v}_L \end{bmatrix}. \quad (4)$$

We first measure the admittance matrix using the conventional approach described in Section II-B. Introducing superscript ‘‘sc’’ for short-circuit we get

$$\mathbf{I}_6^{\text{sc}} = \mathbf{Y}\mathbf{V}_6^{\text{sc}} \quad (5)$$

with

$$\mathbf{I}_6^{\text{sc}} = \mathbf{Y}^{\text{sc}} \quad (6)$$

$$\mathbf{V}_6^{\text{sc}} = \mathbf{E}_6 \quad (7)$$

where \mathbf{E} is the identity matrix.

We next characterize the transformer under open-circuit conditions. We apply voltage vectors \mathbf{v}_H to the HV terminals with the LV terminals open (8a), and measure the current \mathbf{i}_H flowing into the HV side (8b) and the voltage response \mathbf{v}_L at the LV side (8c). $\mathbf{Y}_{H,\text{open}L}$ defines the admittance matrix with respect to the HV terminals while $\mathbf{H}_{\text{open}L}$ defines the voltage transfer from the HV side to the LV side, both with the LV side open. Both matrices are of dimension 3×3

$$\mathbf{i}_L = 0 \quad (8a)$$

$$\mathbf{i}_H = \mathbf{Y}_{H,\text{open}L}\mathbf{v}_H \quad (8b)$$

$$\mathbf{v}_L = \mathbf{H}_{\text{open}L}\mathbf{v}_H. \quad (8c)$$

With the voltage applications \mathbf{v}_H taken as the identity matrix \mathbf{E}_3 , combining (8) with (4) gives

$$\begin{bmatrix} \mathbf{Y}_{H,\text{open}L} \\ \mathbf{0} \end{bmatrix} = \mathbf{Y} \begin{bmatrix} \mathbf{E}_3 \\ \mathbf{H}_{\text{open}L} \end{bmatrix}. \quad (9)$$

The same measurement procedure is repeated with the HV side open. The result is combined with (9) to give (10) which is cast in the compact notation (11)

$$\begin{bmatrix} \mathbf{Y}_{H,\text{open}L} & \mathbf{0} \\ \mathbf{0} & \mathbf{Y}_{L,\text{open}H} \end{bmatrix} = \mathbf{Y} \begin{bmatrix} \mathbf{E}_3 & \mathbf{H}_{\text{open}H} \\ \mathbf{H}_{\text{open}L} & \mathbf{E}_3 \end{bmatrix} \quad (10)$$

$$\mathbf{I}_6^{\text{oc}} = \mathbf{Y}\mathbf{V}_6^{\text{oc}}. \quad (11)$$

Finally, the short-circuit measurement (5) is combined with the open-circuit measurement (11) to give (12), which is written in compact form (13) where subscript ‘‘h’’ denotes hybrid, i.e. both short-circuit (sc) and open circuit (oc)

$$\begin{bmatrix} \mathbf{I}_6^{\text{sc}} & \mathbf{I}_6^{\text{oc}} \end{bmatrix} = \mathbf{Y} \begin{bmatrix} \mathbf{V}_6^{\text{sc}} & \mathbf{V}_6^{\text{oc}} \end{bmatrix} \quad (12)$$

$$\mathbf{I}_h = \mathbf{Y}\mathbf{V}_h. \quad (13)$$

With the proposed approach, one must measure the 6×6 \mathbf{Y}^{sc} as in the conventional method. In addition, one must measure four 3×3 matrices: $\mathbf{Y}_{H,\text{open}L}$, $\mathbf{Y}_{L,\text{open}H}$, $\mathbf{H}_{\text{open}L}$, $\mathbf{H}_{\text{open}H}$. A procedure for measuring these matrices is shown in [12].

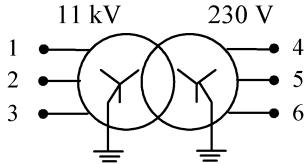


Fig. 2. Two-winding transformer.

B. Calculation of Hybrid Admittance Matrix

Equation (13) is an overdetermined problem since \mathbf{I}_h and \mathbf{V}_h have twice the number of columns than \mathbf{Y} . This equation can be solved as

$$\mathbf{Y} = \mathbf{I}_h \mathbf{V}_h^H (\mathbf{V}_h \mathbf{V}_h^H)^{-1} \quad (14)$$

where superscript H denotes transpose and conjugate. In practice, one will solve (13) in Matlab as $\mathbf{Y} = \mathbf{I}_h / \mathbf{V}_h$ in order to avoid the multiplication $\mathbf{V}_h \mathbf{V}_h^H$ which worsens the condition number.

Since the columns of \mathbf{I} are current responses that come from both short-circuit and open-circuit measurements, they are widely different in magnitude. It is therefore necessary to scale each column i of \mathbf{I} (and \mathbf{V}) such that the columns of \mathbf{I} get about equal norm. In this work, we use the scaling (15). The reason for introducing the square-root in (15) is to avoid inaccurate calculation of \mathbf{Y} in situations where some column in \mathbf{I}_h is extremely small and thus inaccurately measured

$$\alpha_i = \frac{1}{\sqrt{\|\mathbf{I}_i\|_2}}. \quad (15)$$

The extracted \mathbf{Y} is in practice slightly unsymmetrical and so symmetry must be enforced:

$$\mathbf{Y} \rightarrow \frac{\mathbf{Y} + \mathbf{Y}^T}{2}. \quad (16)$$

IV. FREQUENCY-DOMAIN RESULTS

In this section, we compare the performance of the hybrid approach with the conventional approach where the elements of \mathbf{Y} are measured directly.

- 1) Hybrid \mathbf{Y} : Obtained using the procedure in Section III.
- 2) Conventional \mathbf{Y} : Obtained by direct measurement.

The accuracy of the two approaches is assessed by measuring admittance elements and voltage ratios for different terminal conditions:

- 1) all windings grounded;
- 2) one winding grounded, other winding open-circuited;
- 3) two terminals grounded, other terminals open-circuited.

The measured quantities are compared to those computed from the admittance matrices obtained by either the conventional or the hybrid measurement approach.

A. Measurement Setup

The comparison is done for the 300 kVA distribution transformer in Fig. 2. All measurements are done in the range 50 Hz–10 MHz on a logarithmic frequency base using a network analyzer (Anritsu MS4630B) and a measurement setup based on the one shown in [12]. The “connection box” in [12] is used as the reference plane for the measurements.

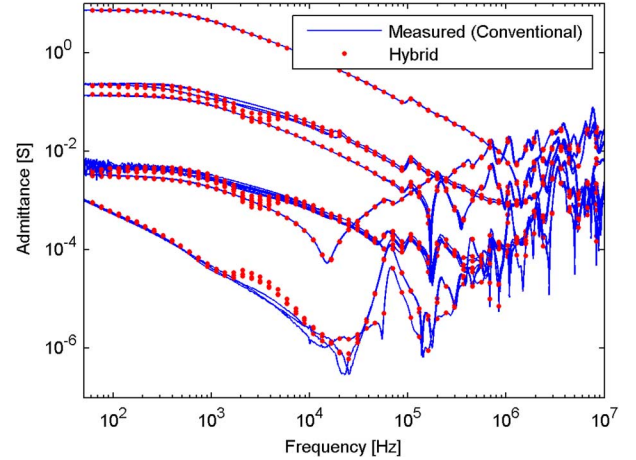
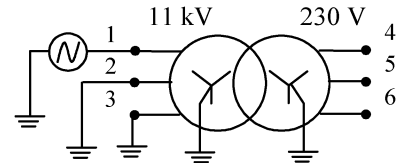
Fig. 3. Elements of \mathbf{Y} .

Fig. 4. Excitation on HV side with open LV side.

B. All Windings Grounded

Fig. 3 compares the directly measured elements of \mathbf{Y} with those obtained by the hybrid method. It is observed that both approaches give a very similar result except for the frequency band 1 kHz–30 kHz where deviations occur. The deviation occurs because the hybrid \mathbf{Y} requires satisfying open-circuit measurements in addition to the short-circuit measurements.

C. Open Low-Voltage Winding

In this test, the voltage is applied alternately to one of the ports 1–3 with ports 4–6 open circuited, see Fig. 4. For this situation, we are interested in the admittance matrix $\mathbf{Y}_{H,openL}$ with respect to the HV side and the voltage ratio from the HV side to the LV side \mathbf{H}_{openL} . These 3×3 matrices are calculated from the full 6×6 \mathbf{Y} by introducing the partition (17). With the condition $\mathbf{i}_L = 0$, the matrices are calculated by

$$\begin{bmatrix} \mathbf{i}_H \\ \mathbf{i}_L \end{bmatrix} = \begin{bmatrix} \mathbf{Y}_{HH} & \mathbf{Y}_{HL} \\ \mathbf{Y}_{LH} & \mathbf{Y}_{LL} \end{bmatrix} \begin{bmatrix} \mathbf{v}_H \\ \mathbf{v}_L \end{bmatrix} \quad (17)$$

$$\mathbf{i}_H = (\mathbf{Y}_{HH} - \mathbf{Y}_{HL} \mathbf{Y}_{LL}^{-1} \mathbf{Y}_{LH}) \mathbf{v}_H = \mathbf{Y}_{H,openL} \mathbf{v}_H \quad (18)$$

$$\mathbf{v}_L = -\mathbf{Y}_{LL}^{-1} \mathbf{Y}_{LH} \mathbf{v}_H = \mathbf{H}_{openL} \mathbf{v}_H. \quad (19)$$

Fig. 5 compares the measured admittance matrix $\mathbf{Y}_{H,openL}$ with the one computed by (18) from either the conventional \mathbf{Y} or the hybrid \mathbf{Y} . It can be seen that the hybrid \mathbf{Y} gives an excellent agreement with the direct measurement of $\mathbf{Y}_{H,openL}$, whereas usage of the conventional \mathbf{Y} gives large errors at frequencies below 10 kHz.

Fig. 6 compares the measured voltage ratio \mathbf{H}_{openL} from high to low with the one calculated from either the conventional \mathbf{Y} or the hybrid \mathbf{Y} . Both approaches produce a good match with the direct measurement although the conventional approach underestimates the voltage ratio of the diagonal (large) elements by

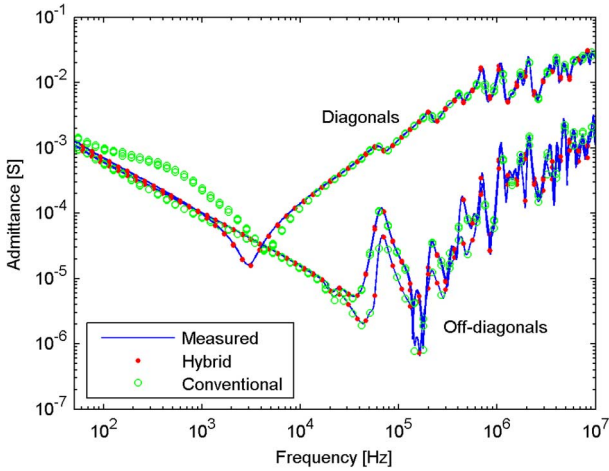


Fig. 5. Elements of $Y_{H,openL}$.

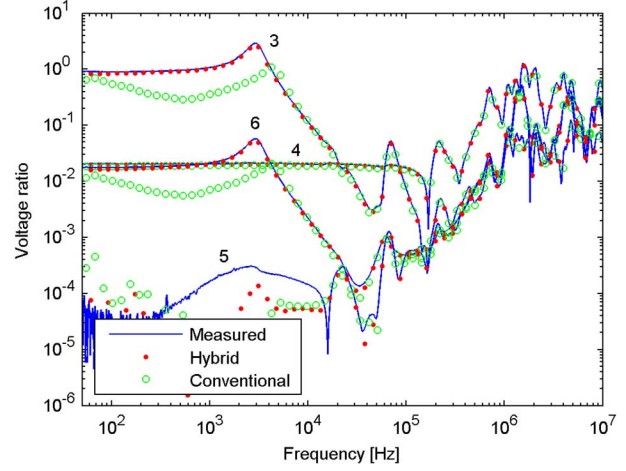


Fig. 8. Voltage transfer for configuration in Fig. 7.

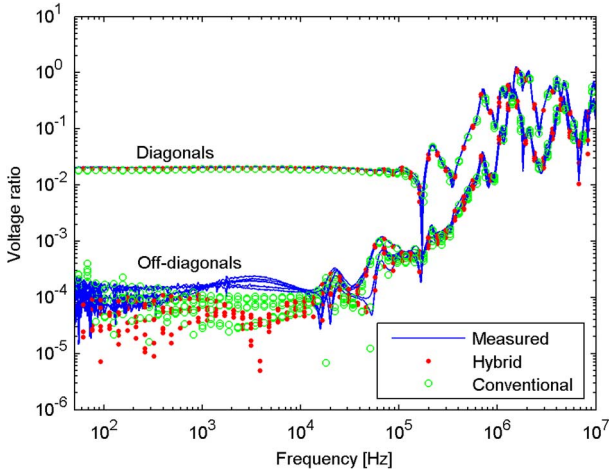


Fig. 6. Elements of H_{openL} .

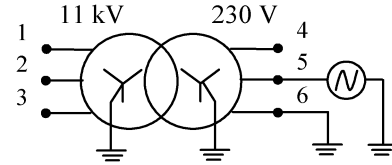


Fig. 9. Excitation on LV side with one LV terminal and HV side open.

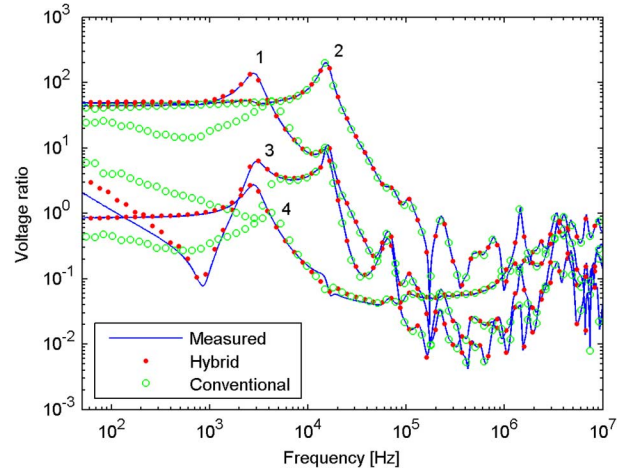


Fig. 10. Voltage transfer for the configuration in Fig. 9.

about 10% at frequencies below 10 kHz. With the hybrid data, the deviation below 10 kHz is smaller than 5%. The accuracy of the off-diagonal elements is less important since they are small and thus represent low voltages.

Similar results were obtained with voltage excitations at the LV side with the HV side open (not shown). The conventional approach gave high errors for $Y_{L,openH}$ at low frequencies and it tended to underestimate the voltage ratio H_{openH} from the LV side to the HV side.

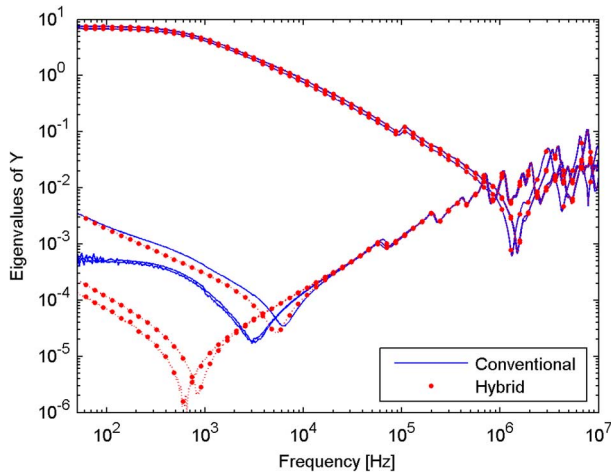
D. Mixed Terminations

We now modify the test with open LV side by removing the grounding of terminal 3, see Fig. 7.

Fig. 8 compares the measured voltage transfer between terminal 1 and terminals 3–6 with the one computed by the conventional Y and the hybrid Y . It is observed that the hybrid measurement produces an excellent result over the full frequency band whereas the conventional approach leads to large errors at frequencies below 10 kHz.

We now modify the test by moving the excitation to the LV side, see Fig. 9.

Fig. 10 compares the measured voltage transfer between terminal 5 and terminals 1–4 with the one computed by the conventional Y and the hybrid Y . Similar to the previous example, the hybrid measurement gives a very good result over the full frequency band while the conventional approach gives a poor result at frequencies below 10 kHz.

Fig. 11. Eigenvalues of \mathbf{Y} .

V. MODAL BEHAVIOR

Fig. 11 shows the eigenvalues of \mathbf{Y} . It is observed that with the hybrid \mathbf{Y} , the eigenvalues are at low frequencies very smooth and two distinct antiresonance points are observed in the two smallest eigenvalues around 1 kHz. The small eigenvalues are with the conventional \mathbf{Y} more irregular at low frequencies and they are missing the two antiresonance points altogether. This result suggests that the hybrid approach is able to represent the small eigenvalues with adequate accuracy while they are corrupted with the conventional approach.

VI. MODEL EXTRACTION

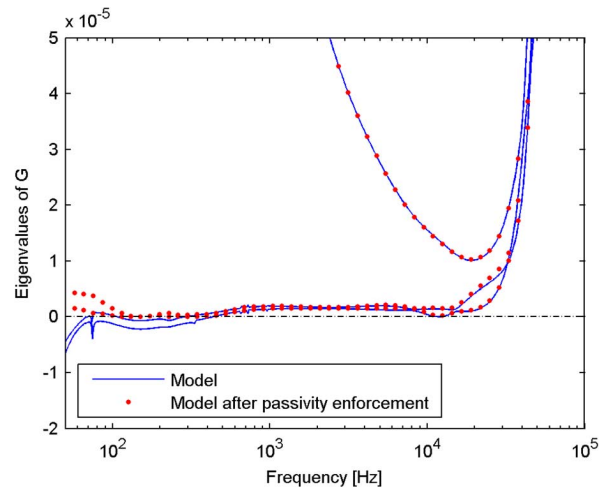
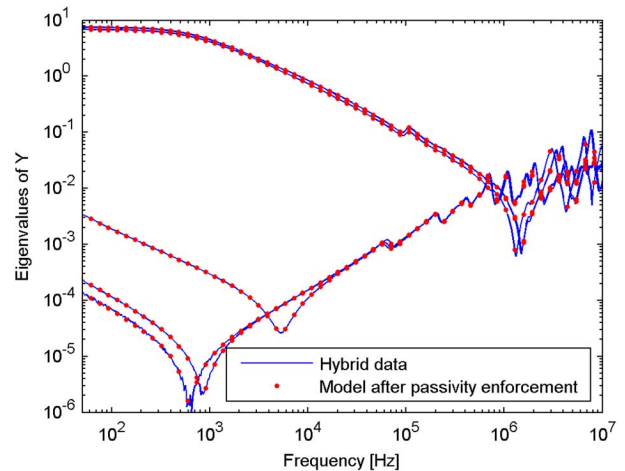
A stable and symmetrical rational model in pole-residue form (20) is extracted by using vector fitting [18] with 100 terms in the sum. In order to retain the accuracy of the small eigenvalues of \mathbf{Y} (Fig. 11), we apply the modal version [17] of vector fitting (MVF). As inverse weighting for the least-squares problems in MVF, we use the square root of the eigenvalue magnitude rather than the eigenvalue magnitude itself. The reason for this modification is to increase the robustness against noise in the data, similar to the weighting (15)

$$\mathbf{Y}(\omega) = \sum_{m=1}^N \frac{\mathbf{R}_m}{j\omega - a_m} + \mathbf{D}. \quad (20)$$

The extracted model is subjected to passivity enforcement based on modal perturbation [19] with residue matrix eigenvalues as free variables [20], and passivity assessment by a half-size test matrix [21], [22]. As inverse weighting for the least-squares part of the constrained optimization problem [20], we use again the square root of the eigenvalue magnitude.

Fig. 12 shows the eigenvalues of $\mathbf{G} = \text{Re}\{\mathbf{Y}\}$ of the model, before and after passivity enforcement. The original model has small passivity violations below 1 kHz since it does not meet the criterion that the eigenvalues of \mathbf{G} are positive. The passivity enforcement is seen to remove the violations.

Fig. 13 compares the eigenvalues of \mathbf{Y} of the hybrid data with those of the passive model. Clearly, a very accurate fitting result has been achieved over the full frequency band.

Fig. 12. Eigenvalues of $\mathbf{G} = \text{Re}\{\mathbf{Y}\}$. Passivity enforcement of the model.Fig. 13. Eigenvalues of \mathbf{Y} after rational fitting and passivity enforcement.

VII. TIME-DOMAIN RESULTS

A. Procedure

As a final test we compare time-domain measurements with simulation results. A step voltage excitation is used in the measurement which is applied as an ideal voltage source in the simulations. Two simulation approaches are compared.

- 1) Hybrid measurement/modeling. The voltage responses are simulated by an EMTP-compatible companion model [23] obtained from the pole-residue model (20) that was extracted from the hybrid \mathbf{Y} in Section VI.
- 2) Conventional measurement. The voltage transfer functions for the considered terminal conditions are calculated in the frequency domain based on the conventional \mathbf{Y} and approximated by rational functions using vector fitting. The time-domain responses are obtained as the (recursive) convolution between the applied voltage and the transfer function impulse response.

B. Excitation on High-Voltage Side

A step voltage is applied to terminal 1 with terminal 2 grounded, see Fig. 7. Fig. 14 shows by solid blue traces the

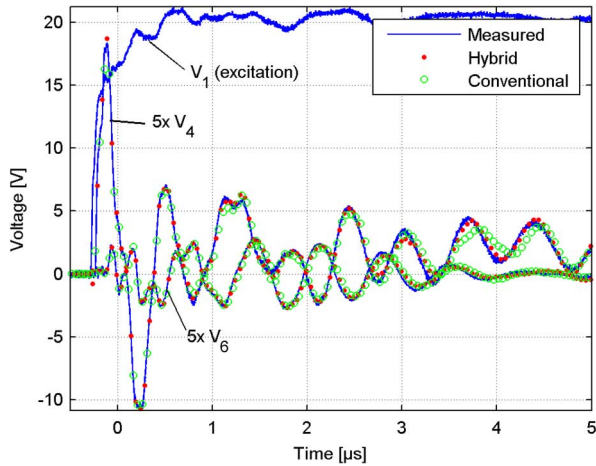


Fig. 14. Step voltage excitation on the HV side. Early response.

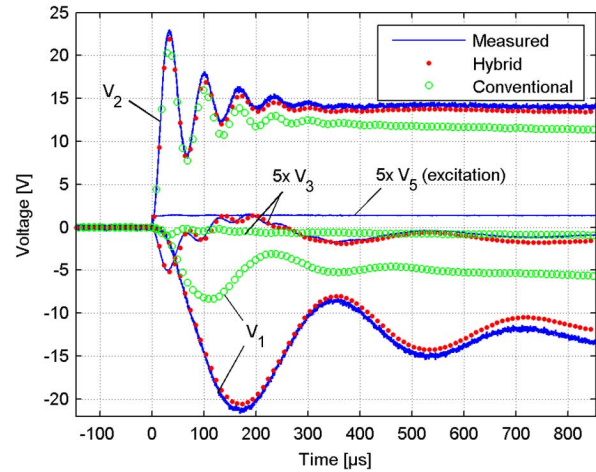


Fig. 16. Step voltage excitation on the LV side.

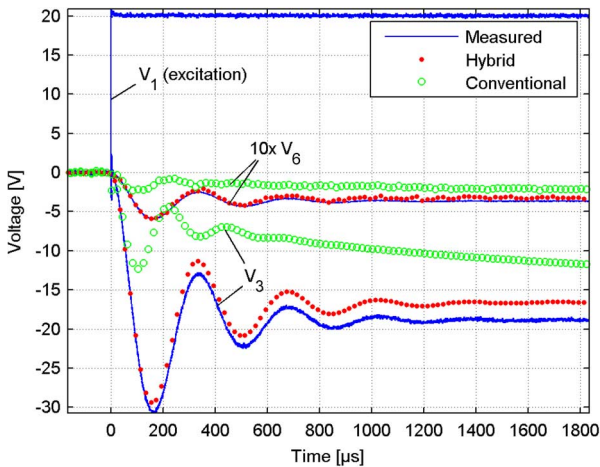


Fig. 15. Step voltage excitation on the HV side. Late response.

applied voltage as well as the voltage response on terminals 4 and 6. The red dots show the simulated voltage responses by the hybrid model while those by the conventional measurement data are shown by green circles. It can be seen that both approaches give excellent results.

Fig. 15 show the response on terminals 3 and 6 when the time range has been increased from 5 μs to 1800 μs . It is seen that using conventional measurement data, a highly incorrect result is obtained for both responses. With the hybrid measurement data, the deviations are much smaller. This result is in complete agreement with the corresponding frequency-domain result in Fig. 8 which shows an inaccurate representation of the voltage responses when characterizing the transformer using the conventional measurement approach.

C. Excitation on the Low-Voltage Side

The test was repeated when the step voltage excitation was moved to the LV side, see Figs. 9 and 16. The results for the voltage responses are similar to those with excitation on the HV side (Fig. 15) in the sense that usage of the hybrid model leads to a great improvement in the calculated results. Again, this result is consistent with the corresponding frequency-domain result (Fig. 10).

VIII. DISCUSSION

A. Accuracy

Although the usage of hybrid data greatly improved the accuracy of the simulation result, the model still gave significant errors when simulating the late response for the excitations as shown in Fig. 15. In order to better understand the reason for the deviation, the response on terminal 3 in Fig. 15 (V_3) was recalculated in two different ways: 1) Convolution with the directly measured voltage transfer function (“Direct data”), and 2) convolution with the voltage transfer function calculated from the Hybrid \mathbf{Y} (“Hybrid data”). The result is shown in Fig. 17.

- 1) Usage of the hybrid model and the hybrid data gives practically the same result. This means that the modeling procedure (rational fitting, passivity enforcement) is not the cause of the deviation.
- 2) Usage of the hybrid data gives a higher deviation than usage of the directly measured frequency response (“Direct data”). This implies that inaccuracies exist in the measurements that the hybrid \mathbf{Y} was calculated from.
- 3) Even the directly measured frequency response gives a notable deviation from the simulated response. One reason for the deviation can be inaccurate frequency-response measurements at low frequencies. Another possible cause is core nonlinear effects as described in [24]. Measuring the output voltage of the VNA and the current monitor using an oscilloscope did indeed reveal distorted waveforms at low frequencies for open-circuit frequency sweep measurements. Regarding the time-domain measurements, we note that the transformer will be driven into saturation if the step voltage excitation is maintained indefinitely. The excitations used in the measurements were of low magnitude but unipolar and in the initial tests also repeated. Some level of saturation may therefore have been present.

B. Reducing the Required Number of Measurements

The hybrid measurement method can be modified in a number of ways by adding or deleting columns from \mathbf{I}_h and \mathbf{V}_h in

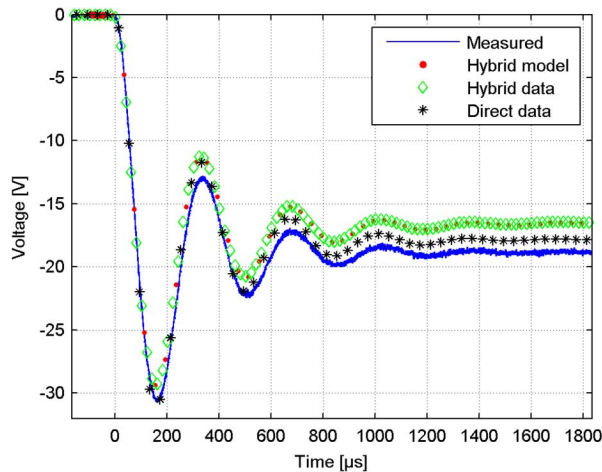


Fig. 17. Voltage response on terminal 1.

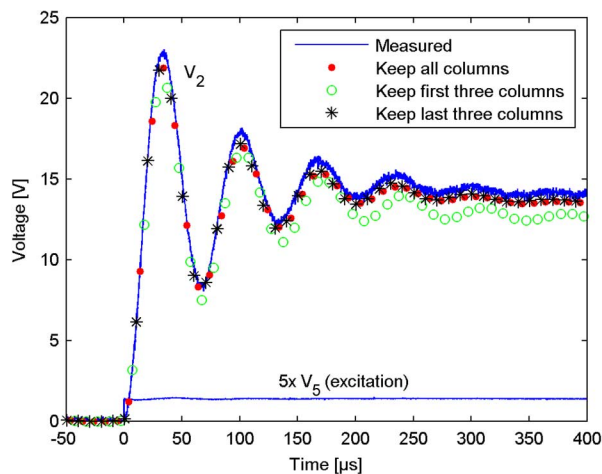


Fig. 18. Voltage response on terminal 2. Deleting columns from **A** and **B**.

(13). Of particular interest is the possibility of deleting vectors in order to reduce the required number of measurements. In what follows, we investigate the consequence of deleting either the first three or last three columns from \mathbf{I}^{sc} , \mathbf{I}^{oc} , \mathbf{V}^{sc} , and \mathbf{V}^{oc} in (12). As a result, \mathbf{I}_h and \mathbf{V}_h become square (6×6). Fig. 18 shows the time-domain response V_2 in Fig. 16, with alternative ways of obtaining \mathbf{Y} . It is observed that keeping all columns or the last three columns gives virtually the same result whereas using only the first three columns gives a somewhat lower voltage. This result is not surprising since in the latter case the open circuit frequency-domain measurements are done with only the LV side open whereas the time-domain measurements (Fig. 18) are done with the HV side open. Conversely, keeping only the last three columns cannot be expected to give a good result with applications involving an open LV winding.

C. Modeling

For the purpose of rational function modeling, it is essential that the hybrid \mathbf{Y} is subjected to a fitting approach based on the modal version of vector fitting (with inverse weighting of

modes). If conventional vector fitting is applied, the small eigenvalues of \mathbf{Y} will tend to become corrupted and error magnifications take place, similarly as when basing the measurements of \mathbf{Y} on (conventional) short-circuit measurements. The error magnification phenomenon due to fitting errors is explained in detail in [17] for application to frequency-dependent network equivalents (FDNEs). For the same reason, it is advantageous to base the passivity enforcement step on modal perturbation [19], [20] in order to prevent the small eigenvalues of \mathbf{Y} from becoming corrupted.

D. Practical Advantages of Hybrid Approach

Although the conventional approach is suitable for most high-frequency transients studies, situations exist where the hybrid approach should be used.

- 1) When the transformer has all terminals of a winding open and at the same time one or more terminals open at the other winding, voltage resonances occur at a few kHz which cannot be reproduced accurately via the conventional approach. The excitations in Figs. 7 and 9 represent such a case. This situation can result when energizing an unloaded transformer in the presence of a stuck breaker pole or a broken conductor.
- 2) Transient interaction between a cable and transformer with unloaded LV winding can in some situations lead to excessive overvoltages on the LV side by resonance. It was shown in a recent study [25] that correct simulation of the phenomenon requires that the admittance seen into the HV side (with open LV side) has to be correctly represented in the model in the relevant frequency band. This admittance is quite accurately represented by the hybrid model as shown in Fig. 5.

E. Physical Considerations

The advantages of the hybrid approach in the low frequency range (below 10 kHz) can also be explained by physical reasoning. While the short circuit measurements give information about winding resistances and leakage inductances, the open circuit measurements provide information about inductances and losses associated with core fluxes. In the situation in Fig. 7 where the third terminal on the HV side is open, a flux will circulate in the core (core surface) between the excited leg and the third leg. The voltage peaks observed in Fig. 8 at 3 kHz are associated with the third leg windings and they coincide with a peak in the excitation current, see Fig. 19. This result suggests that a series resonance takes place between the magnetizing inductance and capacitances associated with the third leg windings. Since the resonance is associated with flux in the core (core surface), nonlinear effects may with this excitation impact the voltage response.

IX. CONCLUSION

This paper has introduced a new procedure for characterizing the terminal behavior of transformers from frequency-response measurements as follows.

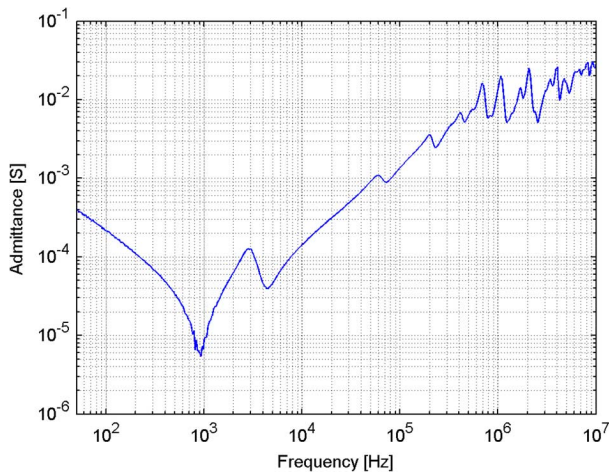


Fig. 19. Admittance seen into terminal 1 with terminal 2 grounded and all other terminals open. Calculated from $\mathbf{Y}_{H,openL}$.

- 1) Short-circuit and open-circuit responses are measured and used for establishing sets of voltage applications and current responses.
- 2) From the voltage applications and current responses, the terminal admittance matrix \mathbf{Y} of the transformer is calculated.
- 3) Frequency-domain measurements show that usage of this hybrid \mathbf{Y} gives information about the transformer behavior which is lost in a direct measurement of \mathbf{Y} . This additional information is essentially contained in the small eigenvalues of \mathbf{Y} and they play an important role in applications involving high-impedance terminations.
- 4) Using modal vector fitting and modal perturbation, the hybrid admittance matrix can be converted into an EMTP compatible simulation model which retains the information about the small eigenvalues of \mathbf{Y} .
- 5) Comparison of simulated results with measured time-domain responses shows that the hybrid model gives substantially more accurate results than a model obtained from a direct measurement of \mathbf{Y} . The improvement occurs in situations where the small eigenvalues of \mathbf{Y} are important and at the same time inaccurately represented in short circuit measurements. This situation is typically encountered with high impedance terminations combined with frequencies below a few tens of kilohertz.

REFERENCES

- [1] H. W. Dommel and W. S. Meyer, "Computation of electromagnetic transients," *Proc. IEEE*, vol. 62, no. 7, pp. 983–993, Jul. 1974.
- [2] J. A. Martinez and B. A. Mork, "Transformer modeling for low- and mid-frequency transients—A review," *IEEE Trans. Power Del.*, vol. 20, no. 2, pt. 2, pp. 1625–1632, Apr. 2005.
- [3] B. A. Mork, F. Gonzalez, D. Ishchenko, D. L. Stuehm, and J. Mitra, "Hybrid transformer model for transient simulation. Part I. Development and parameters," *IEEE Trans. Power Del.*, vol. 22, no. 1, pp. 248–255, Jan. 2007.
- [4] F. De Leon and A. Semlyen, "A complete transformer model for electromagnetic transients," *IEEE Trans. Power Del.*, vol. 9, no. 1, pp. 231–239, Jan. 1994.
- [5] E. Rahimpour, J. Christian, K. Feser, and H. Mohseni, "Transfer function method to diagnose axial displacement and radial deformation of transformer windings," *IEEE Trans. Power Del.*, vol. 18, no. 2, pp. 493–505, Apr. 2003.

- [6] P. G. Blanken, "A lumped winding model for use in transformer models for circuit simulation," *IEEE Trans. Power Electron.*, vol. 16, no. 3, pp. 445–460, May 2001.
- [7] E. Bjerkan and H. K. Høidalen, "High frequency FEM-based power transformer modeling: Investigation of internal stresses due to network-initiated overvoltages," in *Proc. Int. Conf. Power Systems Transients*, Montreal, QC, Canada, Jun. 19–23, 2005, pp. 1–6.
- [8] N. Abeywickrama, Y. V. Serdyuk, and S. M. Gubanski, "High-frequency modeling of power transformers for use in frequency response analysis (FRA)," *IEEE Trans. Power Del.*, vol. 23, no. 4, pp. 2042–2049, Oct. 2008.
- [9] Q. Su, R. E. James, and D. Sutanto, "A z-transform model of transformers for study of electromagnetic transients on power systems," *IEEE Trans. Power Syst.*, vol. 5, no. 1, pp. 27–33, Feb. 1990.
- [10] A. Morched, L. Marti, and J. Ottevangers, "A high frequency transformer model for the EMTP," *IEEE Trans. Power Del.*, vol. 8, no. 3, pp. 1615–1626, Jul. 1993.
- [11] M. J. Manyahi and R. Thottappillil, "Transfer of lightning transients through distribution transformers," in *Proc. Int. Conf. Lightning Protection*, Cracow, Poland, Sep. 2–6, 2002, pp. 435–440.
- [12] B. Gustavsen, "Wide band modeling of power transformers," *IEEE Trans. Power Del.*, vol. 19, no. 1, pp. 414–422, Jan. 2004.
- [13] B. Gustavsen, "Frequency-dependent modeling of power transformers with ungrounded windings," *IEEE Trans. Power Del.*, vol. 19, no. 3, pp. 1328–1334, Jul. 2004.
- [14] M. Tiberg, D. Bormann, B. Gustavsen, C. Heitz, O. Hoenecke, G. Muset, J. Mahseredjian, and P. Werle, "Generic and automated simulation modeling based on measurements," presented at the Int. Conf. Power Systems Transients, Lyon, France, Jun. 4–7, 2007.
- [15] A. Semlyen and A. Dabuleanu, "Fast and accurate switching transient calculations on transmission lines with ground return using recursive convolutions," *IEEE Trans. Power App. Syst.*, vol. 94, no. 2, pp. 561–575, Mar./Apr. 1975.
- [16] SoFT –Simulation of Fast Transients. New service for electrical networks. [Online]. Available: <http://www.abb.com>
- [17] B. Gustavsen and C. Heitz, "Fast realization of the modal vector fitting method for rational modeling with accurate representation of small eigenvalues," *IEEE Trans. Power Del.*, vol. 24, no. 3, pp. 1396–1405, Jul. 2009.
- [18] B. Gustavsen and A. Semlyen, "Rational approximation of frequency domain responses by vector fitting," *IEEE Trans. Power Del.*, vol. 14, no. 3, pp. 1052–1061, Jul. 1999.
- [19] B. Gustavsen, "Passivity enforcement of rational models via modal perturbation," *IEEE Trans. Power Del.*, vol. 23, no. 2, pp. 768–775, Apr. 2008.
- [20] B. Gustavsen, "Fast passivity enforcement for pole-residue models by perturbation of residue matrix eigenvalues," *IEEE Trans. Power Del.*, vol. 23, no. 4, pp. 2278–2285, Oct. 2008.
- [21] A. Semlyen and B. Gustavsen, "A half-size singularity test matrix for fast and reliable passivity assessment of rational models," *IEEE Trans. Power Del.*, vol. 24, no. 1, pp. 345–351, Jan. 2009.
- [22] B. Gustavsen and A. Semlyen, "On passivity tests for unsymmetrical models," *IEEE Trans. Power Del.*, vol. 24, no. 3, pp. 1739–1741, Jul. 2009.
- [23] B. Gustavsen and O. Mo, "Interfacing convolution based linear models to an electromagnetic transients program," presented at the Int. Conf. Power Systems Transients, Lyon, France, Jun. 4–7, 2007.
- [24] N. Abeywickrama, Y. V. Serdyuk, and S. M. Gubanski, "Effect of core magnetization on frequency response analysis (FRA) of power transformers," *IEEE Trans. Power Del.*, vol. 23, no. 3, pp. 1432–1438, Jul. 2008.
- [25] B. Gustavsen, "Study of transformer resonant overvoltages caused by cable-transformer high-frequency interaction," *IEEE Trans. Power Del.*, vol. 25, no. 2, pp. 770–779, Apr. 2010.

Bjørn Gustavsen (M'94-SM'03) was born in Norway in 1965. He received the M.Sc. and Dr.Eng. degrees from the Norwegian Institute of Technology (NTH), Trondheim, Norway, in 1989 and 1993, respectively.

Since 1994, he has been working at SINTEF Energy Research, where he is currently a Senior Research Scientist. His interests include the simulation of electromagnetic transients and modeling of frequency-dependent effects. He spent 1996 as a Visiting Researcher at the University of Toronto, Toronto, ON, Canada, and the summer of 1998 at the Manitoba HVDC Research Centre, Winnipeg, MB, Canada.

Dr. Gustavsen was a Marie Curie Fellow at the University of Stuttgart, Stuttgart, Germany, from 2001 to 2002.